THE CONCEPT OF A NEW CAR SHOCK ABSORBER WITH ENERGY RECUPERATION

KRZYSZTOF SICZEK[1], MACIEJ KUCHAR[2]

Technical University of Lodz

Summary

The concept of a shock absorber able to recuperate from energy chassis vibrations has been presented in the article. Energy released from such vibrations has thus far simply dissipated. The shock absorber is composed of the cylinder, the turbine and the generator. Its dimensions are close to those of hydraulic shock absorber, so the new shock absorber can be used in a typical automobile. The changes for values of dynamic parameters during operation of the new shock absorber components have been estimated using published data. The analysis of dynamics for the shock absorber operating in road conditions has been based on this data. Such analysis has allowed checking the operation correctness of the new design from both the shock absorber and the electric generator point of view. The amount potential of electric power available for recovery in the shock absorber has been estimated for typical road conditions. Such electric power can be used as a comparative parameter in the cost-effectiveness analysis for use of new shock absorbers in automobiles. The model performed of the turbine has been elaborated. Analysis of fluid flows in the model has been carried out and results of it have been shown.

Keywords: shock absorber, energy recuperation, turbine, electric power generator.

Index determinations

A – cross section area of cylinder of the shock absorber, A_1 – cross section area of the upper stator outlet, A_p – pole cross section area, A_Z – magnetic vector potential in Z axis, B – average magnetic flux density, B_r – remanent magnetic flux density, E – electromotive force, H_c – coercive magnetic flux intensity, J_0 – mass polar moment of inertia, L – the blade width, M – moment, N – number of winds of coil, R – mean radius of force loading rotor blade, R_c – circuit resistance, U_A – battery voltage, p – fluid pressure in the cylinder chamber, before the upper stator inlet, r – estimated blade radius, t – time, v – relative rod velocity against the shock absorber cylinder, v_1 – outlet velocity from upper stator, v_2 – peripheral velocity of rotor, v_3 – peripheral velocity of fluid against rotor, α – angle of outlet velocity from upper stator against the rotor axis, ρ – fluid density, ω – angular velocity

[1] Technical University of Lodz, Department of Vehicles and Fundamentals of Machine Design, 116 Żeromskiego Street, 90-924 Lodz, e-mail: krzysztof.siczek@p.lodz.pl, ph.: +48 42 631 22 50

[2] Technical University of Lodz, Department of Vehicles and Fundamentals of Machine Design, 116 Żeromskiego Street, 90-924 Lodz, e-mail: kucharma@p.lodz.pl, ph.: +48 42 631 22 55

1. Introduction

The automobile moving on rough road is loaded by stochastic vertical inputs, which act on its wheel. All of such inputs are independent of each other. Their intensity is proportional to the vehicle speed, almost linearly. Such inputs acting on the automobile wheels initiate vibrations during driving, which are noticed by the driver or passengers as they can create discomfort. Therefore, vehicle designers try to isolate these vibrations from the body by a set of springs and to damp on them by a set of shock absorbers, usually one shock absorber falls on one wheel. In most cases, hydraulic shock absorbers are used in which the energy of vehicle vibrations is precipitated on the flow of hydraulic fluid through the system throttling valves. The energy of the fluid is converted into heat and into used up in the work for overcoming the flow resistance and, therefore, is lost forever.

Such energy, however, may be changed into useful electric power, with the help of additional turbogenerator.

At least part of the energy may be recovered, without significantly decreasing the level of vibration damping, which is provided in most vehicles by classic hydraulic shock absorbers.

The object of research presented in this paper has been a set of hydraulic shock absorber with axial turbine and of electric power generator using permanent magnets.

The aim of the present paper is to investigate the performance of the new shock absorber for different speed of automobile and road conditions.

2. Description of the new hydraulic shock absorber with energy recuperation

The scheme of the new shock absorber has been presented in the Figure 1.

The new shock absorber is composed of the cylinder 1, the turbine assembly 2 and the electric power generator 3. Its dimensions are close to those of hydraulic shock absorber, so the new shock absorber with energy recuperation can be used in the typical chassis of automobile. The turbine assembly can be composed of three stators: upper 2.1, middle 2.2 and bottom 2.3 one or only two stator: upper and bottom one, and of one or two turbine rotors 2.4. The stators are fixed to the bush 2.5 sliding along the inner surface of cylinder 1.1. It is also bearing to the shock absorber rod 1.2. Turbine rotors 2.4 are fixed to the shock absorber rod 1.2 and rotating with it together. The electric power generator is composed of the rotating set of permanent magnets 3.1, made of i.e. Nd-B-Fe, which are fixed to the shock absorber rod 1.2 and of the set 3.2 of poles made from stainless steel and of the set 3.3 of coils made from copper.

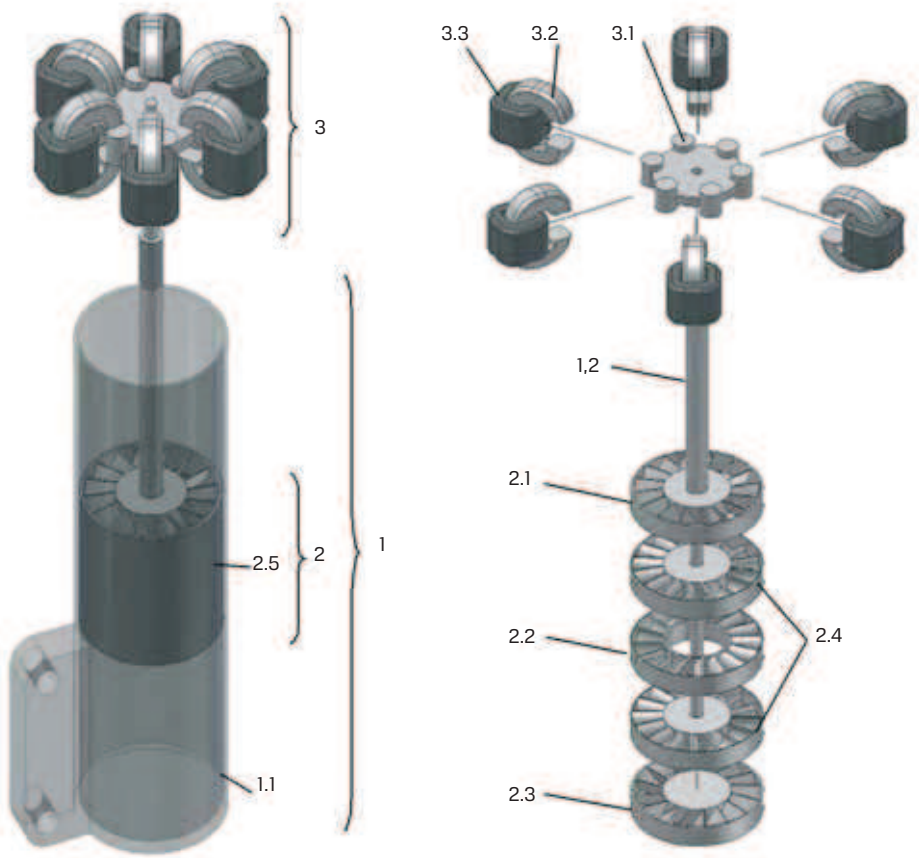

Fig. 1. The scheme of the new shock absorber. 1 – cylinder, 2 – turbine assembly, 3 – electric power generator, 1.1 – inner surface of cylinder, 1.2 - shock absorber rod, 2.1 – upper stator, 2.2 – middle stator, 2.3 – bottom stator, 2.4 – turbine rotor, 3.1 – set of permanent magnets, 3.2 – set of poles, 3.3 – set of coils

3. The model of road roughness and of moving masses for vehicle

The road quality is usually evaluated on the base of the spectral power density for road microprofile. The representative model of road roughness analyzed has been established, basing on the data from [1, 2].

The spectral density of road roughness, for different surface conditions has been shown in the figure 2. The road profile samples have been generated based on such values and using Inverse Fast Fourier Transform, (Fig. 3).

Such values have been used for the excitation of the wheel in the model of moving vehicles. The chassis and the body of the vehicle and its wheels have been modeled as the set

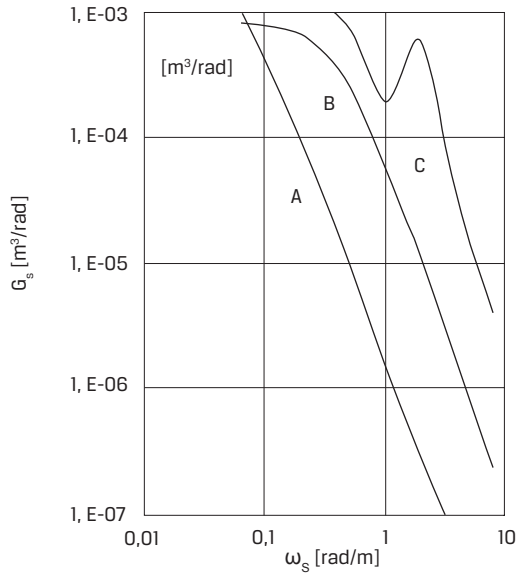

Fig. 2. The spectral density of road roughness G_s vs. relative frequency ω_S: A – asphalt surface in good conditions, B – asphalt surface in poor conditions set of poles, C – paved surface

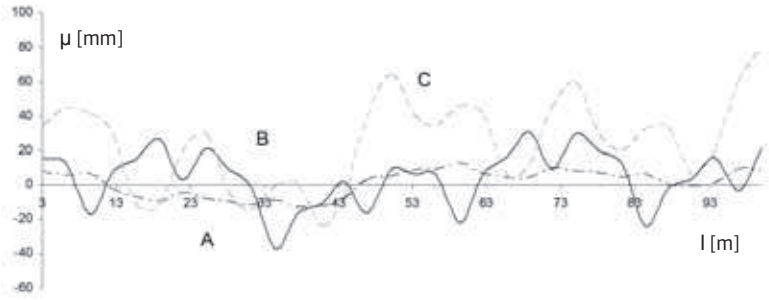

Fig. 3. Road microprofile μ samples generated basing on values of their spectral power density vs. road length l; A – asphalt surface in good conditions, B – asphalt surface in poor conditions, C – paved surface

of two vibrating masses (Figure 4). Such set has been of two degree of freedom. The first mass has been the wheel with the stiffness and damping of its tyre. The second mass has been equal to ¼ of all vehicle mass and it has been associated with the stiffness of the wheel spring and with the nonlinear damping of wheel shock absorber. The characteristic data have been taken from [3].

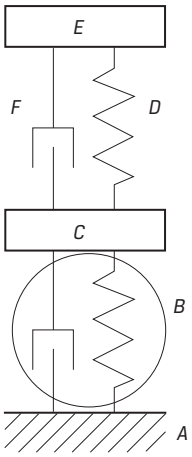

Fig. 4. The modeled set of moving masses for vehicle: the chassis and body and the wheel; A – excitation (vibrations) from road profile, B – tire (stiffness 37 N/mm, damping coefficient 0.15 Ns/mm), C – unsprung mass, D – spring (stiffness 28 N/mm), E - ¼ mass of vehicle (250 kg), F – shock absorber (nonlinear damping coefficient)

4. Analysis on the fluid flow in the turbine assembly

The turbine operates in nonstationary conditions, which makes the analysis of the flow very difficult. Equations for the calculation of axial turbines presented in [8] have been elaborated for conditions of constant rotational velocityof turbine rotor. To simplify the analysis, adiabatic flow of noncompresible hydraulic fluid has been assumed. In reality fluid density can change because of gas bubble initiation or pressure changes. Some heat transfer exists between the fluid and the material of turbine elements, in conditions of high temeprature gradients arising during fluid flow. Such changes are of local character and thus the need to accept the pressure and density values has been recognised, which have been averaged over the time.

The scheme of fluid flow in the turbine assembly has been shown in the figure 5.

The fluid pressure p (fig. 5) in the cylinder chamber, before the upper stator inlet, have been estimated from the equation (1):

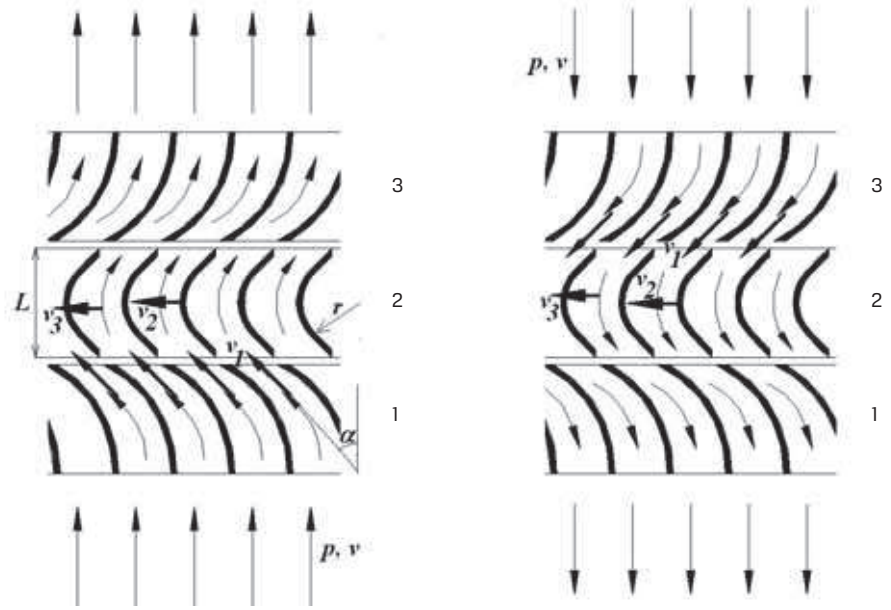

Fig. 5. The scheme of fluid flow in the turbine assembly. 1 – upper stator, 2 – rotor, 3 bottom stator

$$A \cdot v = A_1 \sqrt{p / \rho} \tag{1}$$

where: A = 0.002826 m^2 – cross section area of cylinder of the shock absorber, A_1 = 0.000268 m^2 – cross section area of the upper stator outlet, v = 1 m/s – relative rod velocity against the shock absorber cylinder, p – fluid pressure in the cylinder chamber, before the upper stator inlet, ρ =1000 kg/m^3 – fluid density.

Calculated value of pressure p has been equal 111200 Pa.

The outlet velocity v_1 from upper stator has been calculated from equation (2):

$$v_1 = \sqrt{p / \rho} \tag{2}$$

Calculated value of outlet velocity v_1 has been equal 10.54 m/s.

The peripheral velocity has been calculated from equation (3):

$$v_1 \cdot \cos(\alpha) = v_2 + v_3 \tag{3}$$

where: α = 45° – angle of outlet velocity from upper stator against the rotor axis, v_2 – peripheral velocity of rotor, v_3 – peripheral velocity of fluid against rotor

The moment M loading the turbine rotor has been estimated from the balance of inlet and outlet fluid stream power and turbine power, that has been described by the equation (4):

$$\rho \cdot A_1 \cdot v_1^3 = M \cdot \frac{v_2}{R} + \rho \cdot A_1 \cdot \left(\sqrt{v_3^2 + \left[v_1 \cdot \cos(\alpha) \right]^2} \right)^3 \quad (4)$$

From the second hand the moment M has been calculated from equation (5):

$$M = \frac{\rho \cdot A_1 \cdot L \cdot \left\{ \left[v_1 \cdot \cos(\alpha) \right]^2 + (v_3)^2 \right\}}{r} \cdot R \quad (5)$$

where: r = 0.0105 m – estimated blade radius, R = 0.029 m – mean radius of force loading rotor blade, L = 0.012 m – the blade width.

Calculated value of velocity v_2 has been equal 5.53 m/s, what has corresponded for turbine rotational speed 1820 rpm. The calculated value of velocity v_3 wynosiła 1.93 m/s, has been equal 1.93 m/s, what has corresponded for rotor moment M equal 0.62 Nm. The calculated turbine power has been equal 0.118 kW.

5. Model of electric power generator

The electric power generator utilizes the known phenomenon of EMF generation in coil winds 3.3 on the poles 3.2 (fig. 1), in result of magnetic flux changes in magnetic circuits containing such poles 3.2 [9, 10]. Such changes arise during motion of permanent magnets 3.1 in magnetic circuits, perpendicular to mean symmery planes of the circuits (poles 3.2 – fig. 1). Magnetic flux in such magnetic circuit increases nonlinearly, until peaking and then it decreases almost symmetrically. In order to obtain a higher electric efficiency of generator, its coils can be arranged into the 3-phase set [9, 10]. The model of electric power generator have been made using FEM. To simplify the analysis, the cyclic symmetry concept has been used, so that only a part of electric power generator has been taken into consideration. Such simplification could be supported with the fact of cyclic symmetry existence for the structure of fixed generator, for current flow and for magnetic field gradient. The model consisted of a permanent magnet 4 made of Nd-B-Fe (H_c = 850000 A/m, B_r = 1.2 T), a steel pole 3 and copper coil 2. Such assembly has been positioned in the block of air 1. The analysis has been made for a number of steady angular positions of the permanent magnets assembly in respect to the poles assembly, so it has been analyzed in a steady state only. For reasons of simplicity, the steady-state analysis has been made. It has been assumed, that magnet motion can change values of vector magnetic potential in the assembly, not more than about 5% in comparison to the fixed case. The grid of finite elements has been generated automatically, by commercial program ANSYS [11]. The boundary conditions have been following: on each external surface of the mentioned air block the vector magnetic potential value has been equal zero. The model, finite element grid and boundary conditions have been presented in the Figure 6.

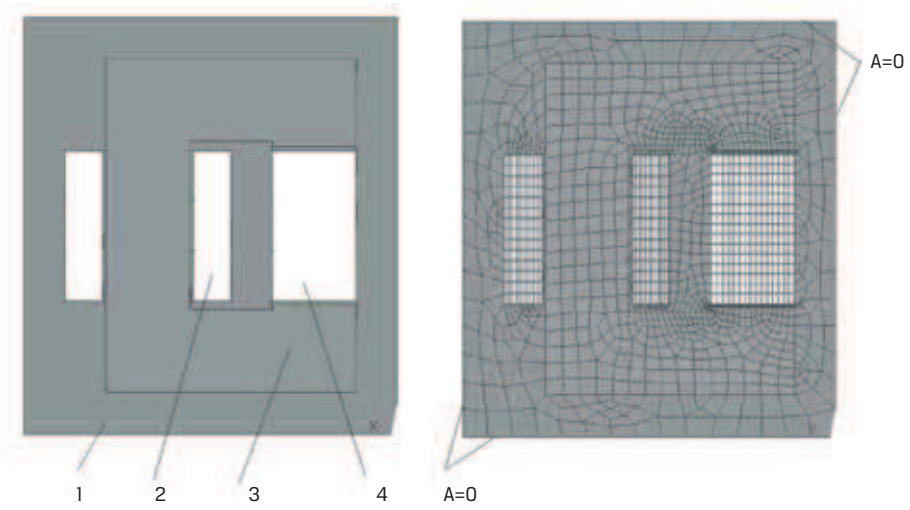

Fig. 6. The model of electric power generator, grid of finite elements and boundary conditions. 1 – air block, 2 – coil, 3 – pole, 4 – permanent magnet

Moment M(t) loading rotor has been calculated from equation (6):

$$M(t) = J_0 \cdot \frac{d\omega}{dt} + \frac{1}{\omega}\left(\mathrm{E} \cdot I + I^2 \cdot R_c\right) = J_0 \cdot \frac{d\omega}{dt} + \frac{1}{\omega}\left(0.5 \cdot N \cdot B \cdot A_p \cdot 3\omega\right) \cdot \left(\frac{0.5 \cdot N \cdot B \cdot A \cdot 3\omega - U_A}{R_c}\right)$$
$$+ \frac{1}{\omega}\left(\frac{0.5 \cdot N \cdot B \cdot A_p \cdot n - U_A}{R_c}\right)^2 \cdot R = J_0 \cdot \frac{d\omega}{dt} + \left(0.5 \cdot 600 \cdot 0.8 \cdot 0.0001 \cdot 3\right) \cdot \left(\frac{0.5 \cdot 600 \cdot 0.8 \cdot 0.0001 \cdot 3 \cdot \omega - 12}{0.6}\right) \quad (6)$$
$$+ \frac{1}{\omega}\left(\frac{0.5 \cdot 600 \cdot 0.8 \cdot 0.0001 \cdot 3 \cdot \omega - 12}{0.6}\right)^2 \cdot 0.6 = J_0 \cdot \frac{d\omega}{dt} + 0.12 \cdot \left(0.072 \cdot \omega - 12\right) + \frac{1}{0.6 \cdot \omega}\left(0.072 \cdot \omega - 12\right)^2$$

where: *J0* – mass polar moment of inertia, *E* – electromotive force, ω – angular velocity, *N* – number of winds of coil, *t* – time, R_c – circuit resistance, *B* – average magnetic flux density, A_p – pole cross section area, U_A – battery voltage

6. Results of calculations

Obtained values of the wheel displacement vs. time and of the relative displacement for the ends of the shock absorber vs. time have been shown in the Figure 6a. Observed delay between such displacements has resulted from the damping existence. Values of the respective relative velocity for the ends of shock absorber have been shown in Figure 6b. They have been of about 0.4 m/s.

The values obtained for the loading of the spring – shock absorber assembly vs. relative velocity for the ends of shock absorber have been shown in the Figure 7.

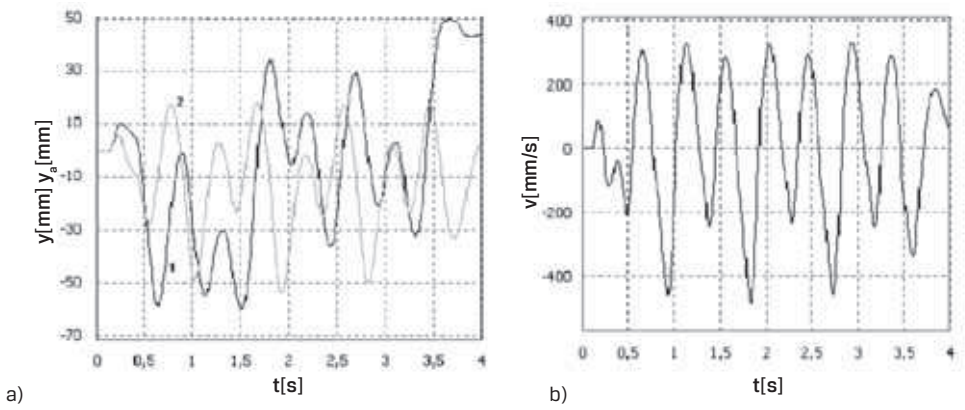

Fig. 7. a) The displacement vs. time 1 - of wheel, 2 - relative for the ends of shock absorber, b) the relative velocity for the ends of shock absorber

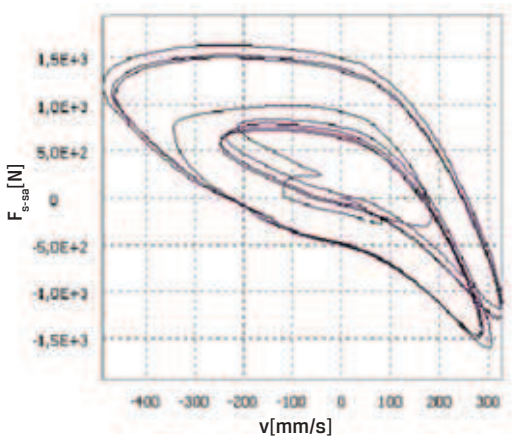

Fig. 8. Loading of the set spring – shock absorber vs. relative velocity for the ends of shock absorber

The irregular shape of such curves has probably resulted from nonlinear damping of shock absorber. As could be predicted the loading of the spring – shock absorber assembly is 3-5 times greater than that of the shock absorber alone. It is similar to the case of the classic hydraulic shock absorber.

Calculated values for the dissipated power during shock absorber operation vs. time have been presented in the Figure 9. The overage value of the power, dissipated during 4 s, has been equal 171 W. The average value of the electrical power received from the turbine rotor, in the same period, was equal 108 W.

The values obtained for rotor angular velocity vs. relative velocity for the ends of shock absorber have been shown in Figure 10. Such curve has been of linear shape. The values obtained of the moment of turbine rotor vs. its angular velocity are presented in the figure 10. Such curve is of parabolic shape. Respective values of the power obtained from turbine rotor have been presented in the figure 12. That curve is of parabolic shape, as well, but of the order three. The values calculated of the force loading the shock absorber during its operation vs. relative velocity for the ends of shock absorber are shown in Figure 13. Such curve is of parabolic shape.

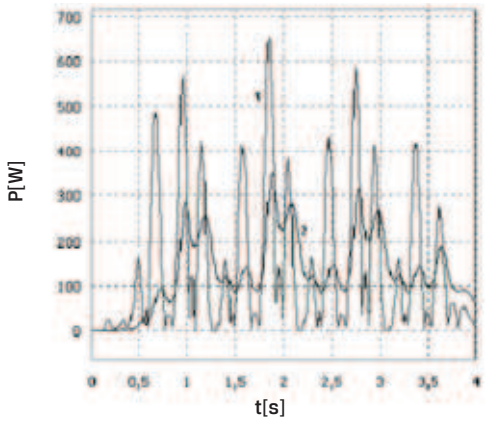

Fig. 9. Power during shock absorber operation vs. time. 1 – dissipated, 2 – electrical received from the turbine rotor of the analyzed shock absorber; paved road, vehicle velocity 100 km/h

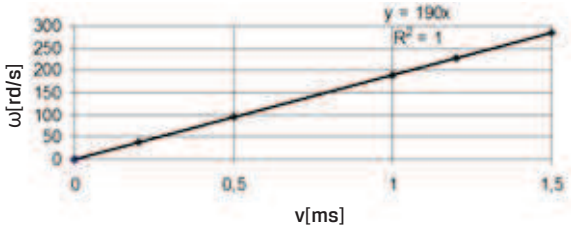

Fig. 10. Rotor angular velocity vs. relative velocity for the ends of shock absorber

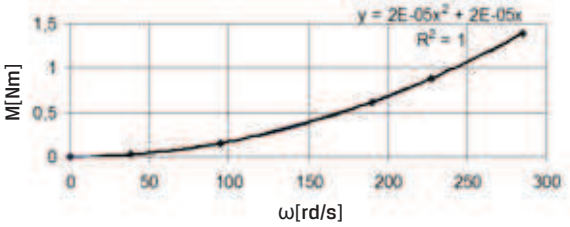

Fig. 11. Moment of turbine rotor vs. its angular velocity

Obtained values of magnet flux density in the pole of generator have been presented in Figure 14. Most of such values were in the range 0.5 – 1 T. The maximum value was equal to 1.635 T and was positioned in the corner of the pole so its value could be predicted.

Obtained values of magnetic vector potential A_z in the set permanent magnet – air gap – pole –air gap in the electric power generator are shown in the Figure 15a (gradient in the outer zone of the set) and 15b (gradient in the inner zone of the set). The values of magnetic vector potential A_z in the other zones of generator model are presented in the Figure 15c. The average values of magnetic vector potential A_z in pole are equal to 0.002 Vs/m.

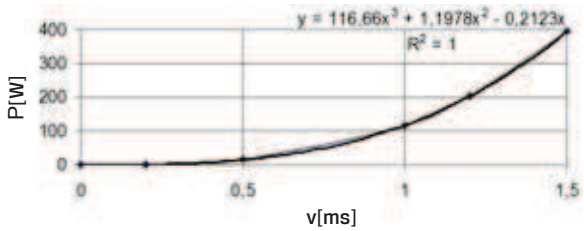

Fig. 12. Power obtained from of turbine rotor vs. relative velocity for the ends of shock absorber

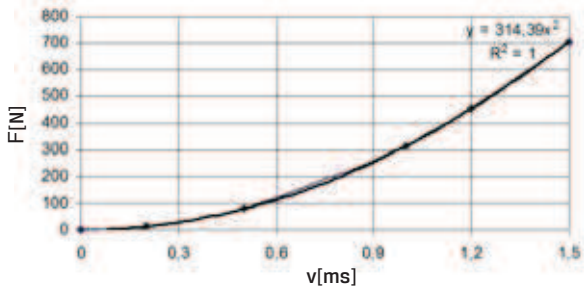

Fig. 13. Force loading the shock absorber vs. relative velocity for the ends of shock absorber

The values calculated for the moment loading rotor and angular velocity of rotor vs. time of rotor operating are presented in the Figure 15. Moment loading turbine rotor remains almost constant during the increase of the rotor angular velocity. Next the moment decreases slowly until the rotor angular velocity obtains its stable value. In the end, such moment decreases rapidly.

7. Conclusions

1. Increasing the number of permanent magnets and coils results in an almost linear increase of the generated emf and of generator efficiency. However, it can increase the generator dimensions simultaneously.

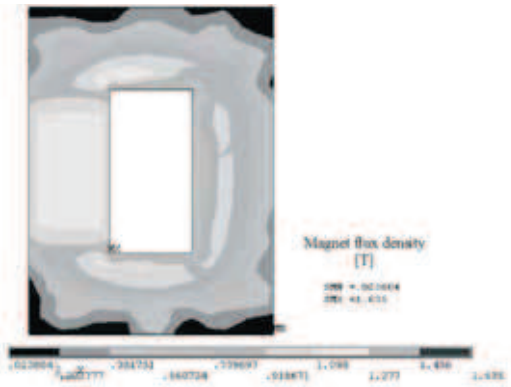

Fig. 14. Magnet flux density in the set permanent magnet – air gap – pole –air gap in the electric power generator

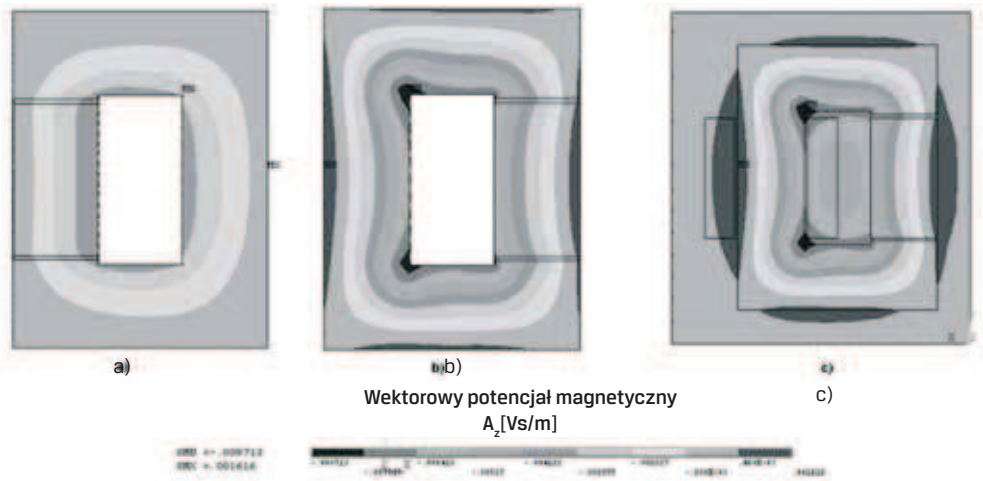

Fig. 15 a) Magnetic vector potential A_z the set permanent magnet – air gap – pole – air gap in the electric power generator; gradient in the outer zone of the set, b) Magnetic vector potential A_z in the set permanent magnet – air gap – pole –air gap in the electric power generator; gradient in the inner zone of the set, c) Magnetic vector potential A_z in the generator model

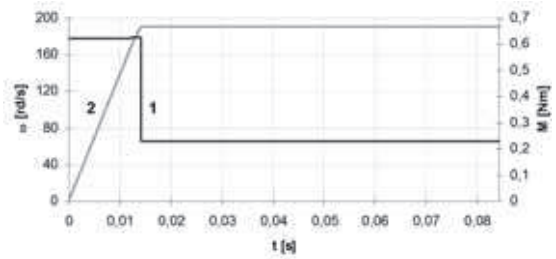

Fig.16. Moment loading rotor *M* and angular velocity of rotor *ω* vs. time *t* of rotor operating

2. Rotor angular velocity increases with the relative velocity for the ends of shock absorber almost linearly.

3. Moment driving the turbine rotor increases with its angular velocity in parabolic way. Respective values of the power obtained from turbine rotor increases in the way of parabolic of the order three.

4. Moment loading turbine rotor is almost constant during begin increasing of the rotor angular velocity, then it decreases slowly until the rotor angular velocity obtains its stabile value. After it, the moment loading turbine rotor decreases rapidly.

5. Force loading the shock absorber during its operation increases with the relative velocity for the ends of shock absorber in the parabolic way.

6. It is possible to obtain a value of electrical power up to 118 W from the described shock absorber.

References

[1] KUCHAR M., SICZEK K.: *Ocena możliwości odzyskiwania energii z układu zawieszenia przy wykorzystaniu amortyzatora pneumatycznego*, Archiwum Motoryzacji 2/2011, pp. 21-37.

[2] AVADHANY S.N.: *Analizes of hydraulic Power Transductin in Regenerative Rotary Shock Absorber as Function of Working Fluid Kinematic Viscosity.* S.B. Materials of Science & Engineering Massachusetts Institute of Technology, 2009.

[3] KAMIŃSKI E., POKORSKI J.: *Dynamika zawieszeń i układów napędowych pojazdów samochodowych,* WKŁ, Warszawa, 1983.

[4] SAYERS M.W., KARAMIHAS S.M.: *The basic information and measurement road profiles,* University of Michigan, 1998.

[5] RAO M.D., GRUENBERG S.: *Measurement of Equivalent Stiffness and Damping of Shock Absorbers,* Michigan Technological University, Houghton, MI 49931, USA.

[6] EMAM M.A.A., SHAABAN S., EL-DEMERDASH S., EL-ZOMOR H.: *A tyre-terrain interaction model for off-road vehicles,* Journal of Mechanical Engineering Research Vol. 3(7), pp. 226-238, July 2011

[7] ŚLĄZKI G., PIKOSZ H.: *Wpływ zmian tłumienia w zakresie zmienności charakterystyki amortyzatora na pionowe obciążenia dynamiczne kół,* Transcomp – XIV International Conference Computer Systems Eided Science, Industry and Transport.

[8] AINLEY D.G., MATHIESONA G.C.R.: *Method of Performance Estimation for Axial-Flow Turbines,* London: Her Majesty's Stationery Office 1957.

[9] PLAMITZER A. M.: *Maszyny Elektryczne,* PWN, Warszawa 1982.

[10] CHEDA W., MALSKI M.: *Silniki,* Wydawnictwo Komunikacji i Łączności, Warszawa 1984.

[11] ANSYS v.12 help on-line documentation.